A Two-Step Synthesis of Broadband Ridged Waveguide Bandpass Filters with Improved Performances

Jean-Christophe Nanan, Jun-Wu Tao, *Member*, *IEEE*, Henri Baudrand, *Senior Member*, *IEEE*, Bernard Theron, and S. Vigneron

Abstract—**A quarter-wave broadband ridged waveguide bandpass filter with improved attenuation has been designed and realized. The two-steps synthesis uses first an equivalent network whose parameters are obtained with a multimodal variational approach which characterizes the discontinuities involved in the structure. It is shown that the frequency behavior of the filter is determined at this step by the chosen filter prototype. The structure is then optimized taking into account all side effects (higher order modes, dispersion), and also the rectangular to ridged waveguides transformer. Predicted data are compared with measured data and a good agreement is observed. It is shown how the use of $\lambda/4$ resonators improves the attenuation in the upper stop-band and reduces the filter volume, which is very important in the aboard satellite telecommunication systems.**

I. Introduction

THE DESIGN of evanescent-mode waveguide filters is now an important topic in the synthesis of passive microwave networks [1]–[4]. Their great attenuation in the upper stop-band combined with the superior electrical performances of ridged waveguide [5] provides a convenient way to realize compact broadband bandpass filters with a sharp selectivity, suitable for use in satellite telecommunication systems [6].

A multimodal variational formulation for the characterization of waveguide discontinuities is used due to its numerical advantages [7], [8]. The design procedure combines this analysis technique with a direct search optimization routine in order to obtain the evanescent-mode ridged waveguide bandpass filter with required performances [7], [9]. However, the determination of initial length for each waveguide section (that is the starting values for optimization routine), plays an important role in the design procedure and constitutes the first step of our work. These values can be obtained by comparing the theoretical coupling coefficient between two waveguide resonators with a chosen J- or K-inverter prototype [4].

Manuscript received April 2, 1991; revised July 26, 1991. J.-C. Christophe, J.-W. Tao, and H. Baudrand are with Laboratoire D'Electronique, ENSEEIHT, 2 rue Camichel, 31071 Toulouse Cedex, France. B. Theron and S. Vigneron are the ALCATEL-ESPACE, 26 rue Champollion, 31037 Toulouse Cedex, France.

IEEE Log Number 9103294.

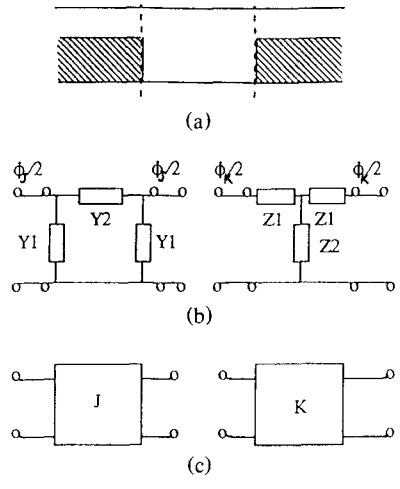

Fig. 1. (a) Symmetrical double discontinuity. (b) Two equivalent networks. (c) Corresponding immittance inverters.

Most of the lowpass and bandpass filters presented in the literature are of half-wave resonator type, which may be bulky in the centimeter-wave range and present a second passband located at about $2f_0$. Thus the stopband attenuation may be not sufficient for multiplexer applications. The originality of this work resides in the design and realization of quarter-wave resonator ridged waveguide bandpass filter. The measured filter performances are in good agreement with the predicted data, showing improved stopband attenuation and the total length of the realized filter has been notably reduced compared to the half-wave filters.

II. Characterization of a Double Discontinuity

A. Variational Formulation

By considering only the dominant-mode incidence, the multimodal variational formulation leads to a 2×2 scattering matrix [7]–[9] from which two reciprocal equivalent networks can be derived, as well as their immittance inverter network representation (Fig. 1). When considering the equivalent T-network case, the reduced impedances can be obtained in the following analytical

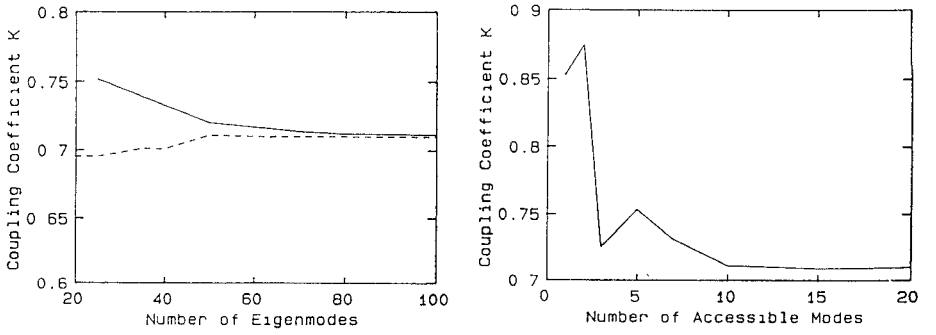

Fig. 2. Convergence behavior versus: (a) number of eigenmodes in the rectangular (—) and the ridged (– –) waveguides; (b) number of accessible modes in the rectangular guide.

forms according to [8]:

$$Z_1 = jX_{\text{odd}}, \quad Z_2 = j(X_{\text{even}} - X_{\text{odd}}) \tag{1}$$

with

$$X_g = -\left|N_1^{(1)}\right|^2 \left(\overline{\overline{Q}}_g^{-1}\right)_{11}, \qquad \boldsymbol{J}_k^{(\nu)} = \boldsymbol{H}_k^{(\nu)} \times z$$

$$N_k^{(\nu)} = \left\langle \boldsymbol{J}_k^{(\nu)}, \boldsymbol{E}_k^{(\nu)} \right\rangle = \int \left(\boldsymbol{J}_k^{(\nu)*} \cdot \boldsymbol{E}_k^{(\nu)}\right) dS$$

$$\left(\overline{\overline{Q}}\right)_{mn} = j \sum_{k=1}^{\infty} \frac{y_{gk}}{N_k^{(2)}} \left\langle \boldsymbol{E}_m^{(1)}, \boldsymbol{J}_k^{(2)} \right\rangle \left\langle \boldsymbol{J}_k^{(2)}, \boldsymbol{E}_n^{(1)} \right\rangle$$

$$y_{gk} = \begin{cases} -j \cdot \cot\left(0.5\beta_k^{(2)} L\right) & g = \text{even} \\ j \cdot \tan\left(0.5\beta_k^{(2)} L\right) & g = \text{odd} \end{cases}$$

L being the inserted waveguide length with β_k the phase constant of kth mode. $\boldsymbol{E}_k^{(\nu)}$ and $\boldsymbol{H}_k^{(\nu)}$ correspond to the transverse electric and magnetic fields of the kth eigenmode in the νth waveguide. Boldface italic letters are used for space vectors.

These relations show clearly how each mode of both waveguides contributes to the value of equivalent network elements. If all modes in the inserted waveguide are below cutoff (it is true in the evanescent-mode filter case), $\overline{\overline{Q}}$ will be a real matrix, then the equivalent network elements will be reactive. In order to insure a good numerical convergence of each circuit element with the mode number in both waveguides, the coupling coefficient between two ridged waveguide resonators, important parameter in the following filter design procedure, has been carried out by using different mode numbers. Fig. 2(a) shows that 50 modes (with only one propagating in 10–44 GHz frequency range) in the propagating ridged waveguide and about 100 modes in the evanescent one will be sufficient for obtaining convergent values. When taking the overall scattering matrix computation during the optimization procedure, (13), (14), (18), and (20) of [8] are used instead of (1). As the filter structure uses the same discontinuity, the individual scattering matrix concerning two semi-infinite waveguides is evaluated only once at each frequency, and the computation time needed to characterize the coupling between two successive discontinuities by considering the notion of accessible modes

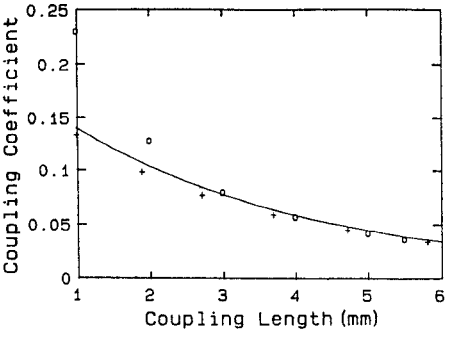

Fig. 3. Coupling coefficient of ridged waveguide resonators versus coupling length. Our results (—) compared with the theoretical (∘ ∘) and measured (+ +) data of [10].

[8], [10] is generally much smaller. In a strong coupling case, about ten accessible modes yield convergent results as shown in Fig. 2(b). However, the convergence test will be needed each time a new structure is used.

This formulation has been applied to the coupling between two ridged waveguide resonators through a bifurcated rectangular waveguide, showing more accurate results than those obtained by the classical variational method [12] (Fig. 3).

B. Immittance Inverter Parameters

The K- and J-inverter type synthesis is preferred to the lumped elements one, because of the dispersive nature of waveguide modes [1]–[4], [13]. The values of such inverter parameters can be easily derived from the T- and π-networks representations. As we know, both types of inverters are needed for a quarter-wave resonator filter design [13], and this means two kinds of waveguide discontinuities, then additional manufacturing and computational efforts will be required. By making use of the two-port network properties, we have shown that in the case of a lossless, symmetrical and reciprocal double discontinuity, the following relations hold (see Appendix):

$$K = J, \qquad \phi_j = \phi_k + \pi. \tag{2}$$

This means that the same discontinuity can be used for either K- or J-inverters, leading to simpler filter structure.

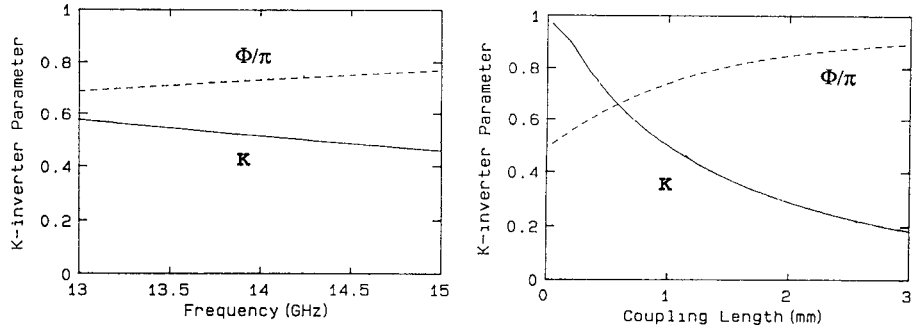

Fig. 4. K-inverter parameters versus (a) frequency and (b) length of evanescent waveguide section.

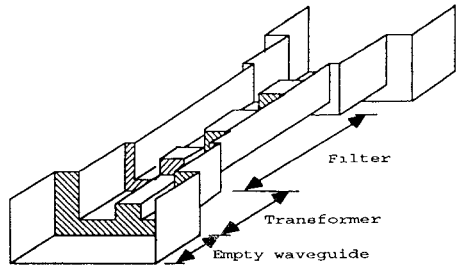

Fig. 5. Evanescent-mode ridged waveguide filter.

A quasi-constant coupling coefficient and a linearly-varying phase correction in the considered frequency range are the key points for a successfully optimized filter design. Fig. 4 shows the behavior of the phase and inversion coefficient versus the frequency (Fig. 4(a)) and the length of waveguide below cut-off (Fig. 4(b)), and we can note that the inverter parameters depend more on the length than on the frequency.

III. Half-Wave and Quarter-Wave Resonator Filters

Since the success of an optimization design depends strongly on the initial parameters (the starting point), we propose here a two-step design procedure:

A first-order design using a well-known bandpass filter prototype (Tchebychev, Butterworth, ...); the waveguide discontinuities are characterized only by their equivalent circuits at the central frequency f_0, the dispersion being neglected. This step allows to determine the starting point for the optimization procedure, and also the filter type. This will be illustrated below by the small difference between the optimized and the first-order design data.

The optimization design procedure in which all the factors (dispersion, ridged waveguide to standard waveguide transformer, etc.) will be considered.

A. First-Order Design

The complete filter structure shown in Fig. 5 can be divided into two parts: the ridged waveguide filter and the stepped rectangular to ridged waveguide transformer. The equivalent network of the filtering section depends on the type of the filter: for the half-wave resonator type, the network is a succession of J-inverters and resonators, while the quarter-wave resonator type is represented by an alternance of K- and J-inverters separated by resonators [13], the section having a K-inverter at its both ends. Owing to the relations (2), the same discontinuity can be used for synthesizing both inverter types. The initial lengths of each section are determined separately for the matching and filtering parts through the following procedure:

1) Determine the central frequency f_0, the number of resonators N and the different inversion coefficients J_n and/or K_n by using a classical prototype from the filter specifications [13]:

$$J_{01}, K_{01} = \sqrt{\frac{\alpha}{2}\frac{\delta\bar{\omega}}{g_0 g_1}} = J_{N,N+1}, \quad K_{N,N+1}$$

$$J_{l,l+1}, K_{l,l+1} = \frac{\alpha \cdot \delta\bar{\omega}}{2}\sqrt{\frac{1}{g_l g_{l+1}}}, \quad 1 \leqslant l \leqslant N-1 \quad (3)$$

with

$$\alpha = \begin{cases} \pi & \text{for half-wave resonator type} \\ \pi/2 & \text{for quarter-wave resonator type} \end{cases}$$

2) Identify the initial lengths of evanescent waveguide sections which provide the required inversion coefficients at f_0, by using the rigorous discontinuity characterization described above. The values of ϕ_n can then be derived.

3) Determine the initial resonator lengths:

$$L_l = \frac{\lambda_g}{2\pi}\left[\alpha + 0.5(\phi_{l-1,l} + \phi_{l,l+1})\right], \quad 1 \leqslant l \leqslant N. \quad (4)$$

4) Determine the number and initial lengths of a stepped quarter-wave rectangular to ridged waveguide transformer in the same way.

B. Second-Order Design

This step consists in minimizing the following error function:

$$\Psi(\bar{L}) = \sum_i \left|S_{11}(\bar{L}, f_i)\right|^2 + \sum_j \left|S_{12}(\bar{L}, f_j)\right|^2. \quad (5)$$

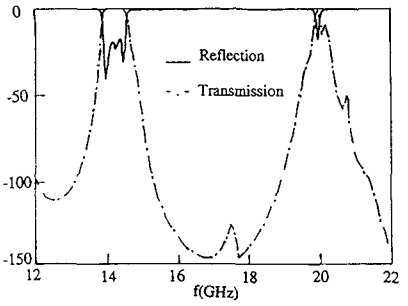

Fig. 6. Predicted scattering parameters in dB for an optimized half-wave resonator bandpass filter.

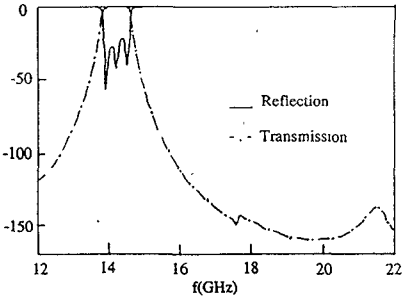

Fig. 7. Predicted scattering parameters in dB for an optimized quarter-wave resonator bandpass filter.

TABLE I
DEVIATION OF OPTIMIZED FILTER DATA FROM THE FIRST-ORDER DESIGN DATA

	$R_0 = R_7$	$I_{01} = I_{67}$	$R_1 = R_6$	$I_{12} = I_{56}$	$R_2 = R_5$	$I_{23} = I_{45}$	$R_3 = R_4$	I_{34}
First-order data (mm)	7.62	2.27	1.76	6.23	1.33	6.88	1.32	7.50
Optimized data (mm)	7.29	2.34	1.75	6.23	1.33	6.86	1.32	6.97

R denotes resonator sections and I for immittance inverters.

f_i, f_j correspond to the sample frequencies within the passband and the stopband respectively and $\bar{L}$ is the vector containing all the waveguide lengths to be optimized. In the following examples, $\bar{L}$ will be a ten elements vector for an eight-resonator bandpass filter with two step transformers, by considering the structure symmetry. The overall scattering matrix is obtained by applying the multimodal variational formulation to the overall filter structure including the step transformer. The result of the first order design is used as the starting point in this procedure, allowing more efficient minimum point search in which the final lengths of the complete filter will be determined.

C. Numerical and Experimental Results

In order to demonstrate the advantages of $\lambda/4$ resonator filter over the $\lambda/2$ resonator one, two ridged waveguide bandpass filters have been designed in the Ku-band by using both resonator types. The optimized reflection and transmission coefficients are given in Figs. 6 and 7. Considerable improvement of the stopband attenuation has been observed in the $\lambda/4$ resonator filter case, as expected, facilitating its use in the multiplexer design.

The difference between the first-order design data and the optimized data has been given in Table I for the $\lambda/4$ resonator filter, showing only slight deviations except for the lengths of the strongest and the smallest coupling sections. It will be noted that the overall filter length of the $\lambda/4$ resonator filter is 76 mm, compared to the 200 mm for the $\lambda/2$ resonator one.

The stability of the minimum will be very critical in a multivariable (for instance 10) optimization procedure. For this reason the study of sensitivity has been carried out for two cases. In the first, the inverter lengths have been increased by 10 μm while those of resonators are decreased by 10 μm (Fig. 8(a)); in the second, the gap between the ridge and the waveguide wall is 0.58 mm instead of 0.6 mm (Fig. 8(b)). No obvious deterioration of filter performances is observed, but the mechanical errors, especially those on the ridge depth, introduce a significant frequency shift (100 MHz for 20 μm error on ridge depth).

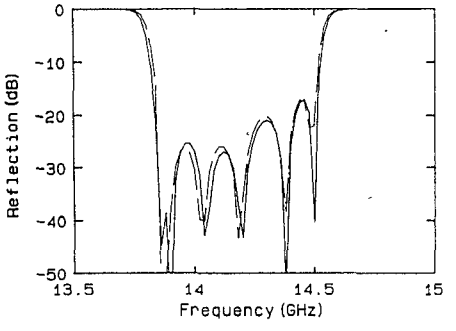

(a)

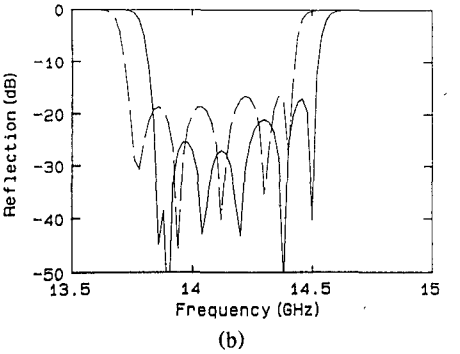

(b)

Fig. 8. Sensitivity studies on an optimized $\lambda/4$ resonator bandpass filter. (a) With all inverter lengths increased by 10 μm and those of resonators decreased by 10 μm (−.−); (b) With the gap between ridge and waveguide wall changed from 0.6 mm (—) to 0.58 mm (−.−).

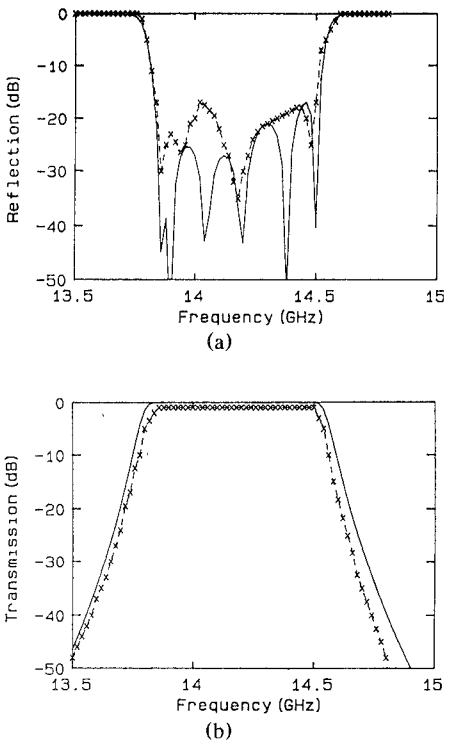

Fig. 9. Comparison between predicted (—) and measured (xx). (a) Return losses. (b) Transmission losses of a $\lambda/4$ resonator ridged waveguide bandpass filter.

A prototype of quarter-wave resonator bandpass filter has been realized by ALCATEL-ESPACE according to the optimized data. The measured reflection and transmission coefficients agree well with the predicted data as shown in Fig. 9. However, tuning screws have been placed in the ridge of each step transformer section, because of the sensitivity of ridge depth described earlier.

IV. Conclusion

A two-step filter synthesis has been described, which combines a first-order synthesis, based on an equivalent network representation of the structure, with an optimization procedure associated with a rigorous multimodal variational analysis. It is shown that the first step allows not only a fast minimum research in the optimization procedure, but also, and above all, to choose the filter type by using the prototype and resonator type which corresponds more closely to the practical requirements. On the other hand, the use of multimodal variational method allows the integration of a rigorous full-wave discontinuity analysis in a multivariable optimization procedure implemented on a personal computer, owing to the numerical advantages of this approach as we have already discussed in other papers.

The application of this design procedure on both $\lambda/2$ and $\lambda/4$ resonator ridged waveguide bandpass filter has shown that better stopband attenuation can be obtained by using the $\lambda/4$ resonator filter design, and the realized *Ku*-band filter is more compact, then more convenient for its use in satellites. It will be noted that the proposed design procedure can be applied to other filter structures [9].

Appendix
Relations between J- and K-Inverter Parameters

The S-matrix of a double discontinuity can be derived from the T- and π-equivalent networks (Fig. 1):

$$Z_1 = \frac{1 - S_{12} + S_{11}}{1 - S_{11} + S_{12}}, \quad Z_2 = \frac{2S_{12}}{(1 - S_{11})^2 - S_{12}^2}$$

$$Y_1 = \frac{1 - S_{12} - S_{11}}{1 + S_{11} + S_{12}}, \quad Y_2 = \frac{2S_{12}}{(1 + S_{11})^2 - S_{12}^2}. \quad \text{(A1)}$$

The corresponding immitance inverter can then be easily deduced:

$$\phi_K = -\tan^{-1}(2Z_2 + Z_1) - \tan^{-1}Z_1,$$
$$K = \left|\tan\left(\phi_K/2 + \tan^{-1}Z_1\right)\right|$$
$$\phi_J = -\tan^{-1}(2Y_2 + Y_1) - \tan^{-1}Y_1,$$
$$J = \left|\tan\left(\phi_J/2 + \tan^{-1}Y_1\right)\right|. \quad \text{(A2)}$$

If we consider a lossless, reciprocal and symmetrical two-port, the scattering matrix will be unitary and the following relations hold:

$$S_{11}S_{11}^* + S_{12}S_{12}^* = 1$$
$$\mathrm{Re}(S_{11})\,\mathrm{Re}(S_{12}) + \mathrm{Im}(S_{11})\,\mathrm{Im}(S_{12}) = 0. \quad \text{(A3)}$$

Here $\mathrm{Re}(z)$ and $\mathrm{Im}(z)$ denote the real and imaginary parts of z. One obtains from (A3)

$$a = \frac{\mathrm{Im}(S_{11}) + \mathrm{Im}(S_{12})}{1 - \mathrm{Re}(S_{11}) - \mathrm{Re}(S_{12})} = \left[\frac{\mathrm{Im}(S_{11}) + \mathrm{Im}(S_{12})}{1 + \mathrm{Re}(S_{11}) + \mathrm{Re}(S_{12})}\right]^{-1}$$
$$b = \frac{\mathrm{Im}(S_{11}) - \mathrm{Im}(S_{12})}{1 - \mathrm{Re}(S_{11}) + \mathrm{Re}(S_{12})} = \left[\frac{\mathrm{Im}(S_{11}) - \mathrm{Im}(S_{12})}{1 + \mathrm{Re}(S_{11}) - \mathrm{Re}(S_{12})}\right]^{-1} \quad \text{(A4)}$$

so we have from (A1), (A2), and (A4)

$$\phi_K = -\tan^{-1}(a) - \tan^{-1}(b)$$
$$\phi_J = -\tan^{-1}\left(\frac{1}{a}\right) - \tan^{-1}\left(\frac{1}{b}\right) = \phi_K + \pi$$
$$K = \left|\tan\left(0.5\left(-\tan^{-1}(a) + \tan^{-1}(b)\right)\right)\right|$$
$$J = \left|\tan\left(0.5\left(\tan^{-1}(a) - \tan^{-1}(b)\right)\right)\right| = K. \quad \text{(A5)}$$

References

[1] G. F. Craven and C. K. Mok, "The design of evanescent mode waveguide bandpass filter for a prescribed insertion loss characteristic," *IEEE Trans. Microwave Theory Tech.*, vol. MTT-19, pp. 295–308, Mar. 1971.

[2] C. K. Mok, "Design of evanescent mode waveguide diplexers," *IEEE Trans. Microwave Theory Tech.*, vol. MTT-21, pp. 43–48, Jan. 1973.
[3] R. V. Snyder, "Broadband waveguide or coaxial filters with wide stopbands, using a stepped-wall evanescent mode approach," *Microwave Journal*, pp. 83–88, Dec. 1983.
[4] L. Q. Bui, D. Ball, and T. Itoh, "Broadband millimeter-wave E-plane bandpass filters," *IEEE Trans. Microwave Theory Tech.*, vol. MTT-32, pp. 1655–1658, Dec. 1984.
[5] S. B. Cohn, "Properties of ridged waveguide," *Proc. IRE*, vol. 35, pp. 783–788, Aug. 1947.
[6] A. M. K. Saad et al., "Evanescent-mode serrated ridged waveguide bandpass harmonic filters," in *Proc. 16th. European Microwave Conf.*, Dublin, Ireland, 1986, pp. 287–291.
[7] J. W. Tao and H. Baudrand, "New design procedure for evanescent-mode ridged waveguide filters," in *Proc. 1989 URSI EM Theory Symp.*, Stockholm, Sweden, 1989, pp. 458–460.
[8] J.-W. Tao and H. Baudrand, "Multimodal variational analysis of uni-axial waveguide discontinuities," *IEEE Trans. Microwave Theory Tech.*, vol. 39, pp. 506–516, Mar. 1991.
[9] P. Couffignal, J-C. Nanan, J.-W. Tao, H. Baudrand, and B. Theron, "A multimodal variational approach for the characterization of waveguide discontinuities for microwave filter design," in *Proc. 20th European Microwave Conf.*, Budapest, Hungary, 1990, pp. 919–924.
[10] T. E. Rozzi and W. F. G. Mecklenbralker, "Wide-band network modeling of interacting inductive irises and steps," *IEEE Trans. Microwave Theory Tech.*, vol. MTT-23, pp. 235–245, Feb. 1975.
[11] A. S. Omar and F. Schünemann, "Transmission matrix representation of finline discontinuities," *IEEE Trans. Microwave Theory Tech.*, vol. MTT-33, pp. 765–770, Sept. 1985.
[12] Y. Konishi, "Planar circuit mounted in waveguide used as downconverter," *IEEE Trans. Microwave Theory Tech.*, vol. MTT-26, pp. 716–719, Oct. 1978.
[13] G. L. Matthaei, L. Young, and E. M. T. Jones, Microwave filters, impedance matching networks and coupling structures. New York: McGraw-Hill, 1964.

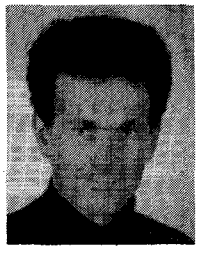

Jean-Christophe Nanan was born in Nancy, France, in 1965. He received the Diplôme d'Ingénieur degree and the DEA degree in electronics from ENSEEIHT, Toulouse, France, in 1988.

Since then he has been doing research work on waveguide discontinuity problems and microwave filter design in the Electronics Laboratory of ENSEEIHT, where he is pursuing Ph.D. studies. Actually he is with CERN (European Organization for Nuclear Research), Genève, where he is working on the accelerating cavity.

Jun-Wu Tao (M'91) was born in Hubei, China, in 1962. He received the B.Sc. degree in electronics from the Radio Engineering Department, Hua Zhong (Central China) University of Science and Technology, Wuhan, China, in 1982 and the Ph.D. degree from the Institut National Polytechnique of Toulouse, France, in 1988.

Since then he has been doing postdoctoral research in the Electronics Laboratory of ENSEEIHT in Toulouse, France. His main research interest is the application of various numerical methods to two- and three-dimensional boundary condition problems in electromagnetics, including propagation in inhomogeneous and anisotropical waveguides and planar waveguides, discontinuity modelling in scattering and radiating structures, and the design of microwave and millimeter-wave devices.

Dr. Tao received a Chinese Overseas Graduate Scholarship in 1982. His Ph.D. dissertation received the Leopold Escande Prize in 1989.

Henri Baudrand (M'86–SM'90), for photograph and biography, see this issue, p. 2129.

Bernard Theron was born on December 18, 1950. He graduated with a degree in electrical engineering in 1975.

From 1977 to 1978 he worked at CNET (French Telecommunications Laboratory) on PCM/PSK systems. In 1978 he joined the Thomson-CSF Microwave Links Division to work on antenna systems. From 1980 to 1984 he was an engineer at Thomson-CSF and then at the Alcatel Espace Microwave Laboratory. He worked on the design and development of microwave filters for telecommunications satellites (TELECOM 1, TDF, TELE-X, INTELSAT VI, EUTELSAT-II) and miscellaneous R&D programs. From 1985 to 1988 he was Manager of the Passive Microwave Laboratory at Alcatel Espace and was in charge of passive R&D studies. He is now the Manager of the Receivers and Filters Laboratory at Alcatel Espace, Toulouse, France.

S. Vigneron was born in Limoges, France, in December 1958. He received the doctor degree in electrical engineering in 1988 from the University of Limoges.

Since 1988 he has been a Design Engineer in the repeaters product line of Alcatel Espace, Toulouse, France. He worked on the design and the development of *L*-band dielectric resonators power diplexer (CNES contract) and *Ku*-band filters for active antennas (French Telecommunications contract). His current work is in the study and the design of the output multiplexers for telecommunications satellite TURKSAT.